Electric Control LoadingSystem Control Strategy Study Based on LMI

YupingWang[1], QingweiMeng[2] and XuriTang[1]

[1]*Heilongjiang University of Science and Technology, China,*
[2]*Harbin University of Science and Technology, China*
wangyupinghkj@126.com

Abstract

Electric Control Loading System is to provide drivers with force feedback force displacement following system, the inner-loop as force-loop limited by strong disturbance of position loop and the narrow system frequency width, cause the system dynamic response is poor and simulation effect of force is bad. How to retrain disturbance of position loop surplus force and expand force loop bandwidth isa key problem for this system. This paper establishedthe physical and mathematical model of motor type electric control loading system, described the method to determine the parameters of force loop(inner loop) model; According to the characteristicsof force loop, the controller of force loop was designed based on LMI(linear matrix inequality), semi-physical simulation show that the controller restrain effectively the disturbance of surplus force, extend the bandwidth and improve rapid response of force loop. and user feedback showed that Electric Control Loading System's static and dynamic characteristics fully meet the standardmilitarysimulatorwith this paper's control strategy.

Keywords: flight simulator; electric control load; parameter identification; LMI robust control;semi-physical simulation

1. Introduction

Flight simulator is a real-time simulation system of man in the loop, the control loading system is used to simulate the pilot's force sensing as manipulate real aircraft. Full digital control electric control loading system has technical and cost advantage than hydraulic system, became an ideal choice for large simulator [1]. The electric control loading system of a company in Holland is currently the most widely used and most high-end products, torque motor, reducer and feedback sensors of the system are custom-made, the system performance is excellent, but high price ,inconvenient repair, complex operation. So we decide to develop high performance to price ratio control loading system.

In this paper, the torque sever motor is used as power actuator, coupled with theconventional speed reducer and force sensor constructed electric control loading system. This paper describes how to establish mathematical model of control loading system, the controller based on linear matrix inequality restrain the surplus force disturbance generated by thepositiondisturbance, effective compensation within the inner-loop bandwidth. The control loading system achieves good simulation effect.

2. System Models and Control Strategy

Considering installation space and power requirement, the control loading system adopt with servo motor and reducer structure, reducer convert small torque and high speed of servo motor to high torque low speed, that match the low speed and vigorously handle of the operating mechanism, the output shaft of the reducer are connected with the driving mechanism through rocker arm and connecting rod. Composition of electric control loading system is shown in Figure 1 a).
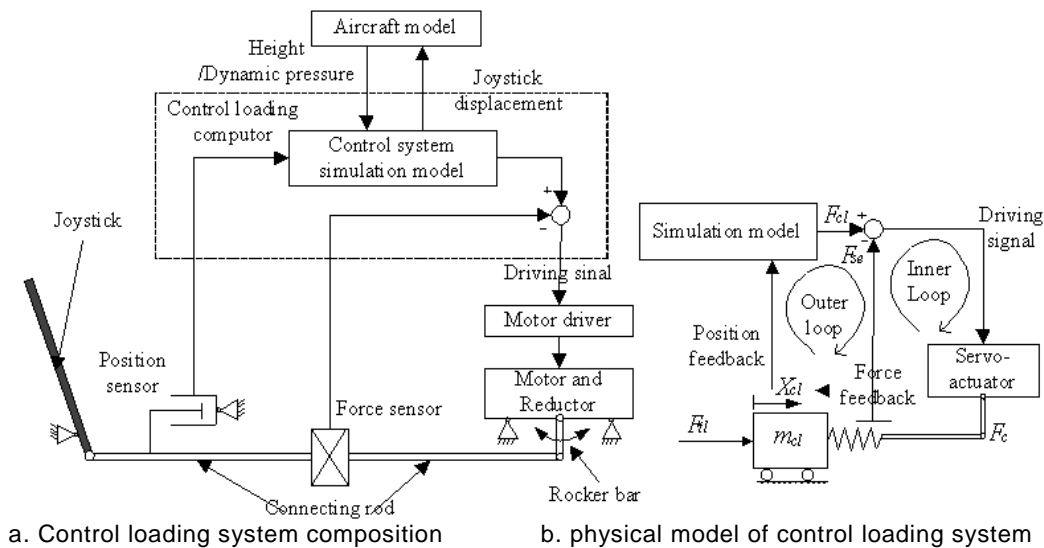

a. Control loading system composition   b. physical model of control loading system

Figure 1. Electric Control Loading System Components and Equivalent Model

The control of control loading system mainly have the position loop, speed loop and force loop three mode that the domestic and foreign scholars have studied, the force loop control is relatively good, and the most widely used [2-3]. The model of electric control loading system [4-5] is shown in Figure 1 b) based on force loop mode consists of two parts: the aircraft manipulation system model that produce force displacement curve, also called the outer loop which contains operating mechanism, simulation model, displacement sensor and inner loop; another is the electric servo loading system model, also called the inner loop that contains force sensor, servo drive and electric actuator.

2.1. The Outer Loop Model

The outer loop is used to determine the load force that the pilot felt. The main input of outer loop is the manipulation displacement; the main output is generated to force. The outer loop model relate to the plane model and flight status, the typical joystick displacement and force curve as shown in Figure 2, positive and negative travel force difference is caused by the friction of the operating mechanism, starting force is not zero in middle position.
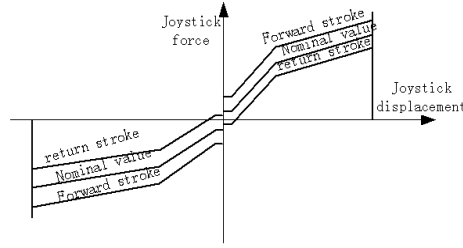

Figure 2. Typical Driving Force - Displacement Curve

2.2. The Inner Loop Model and Parameter Identification

The motor load object can be simplified as two elastic link qualities after connection force sensor serially in linkage mechanism, the first mass is rotor ,rocker arm and some linkage in front of force sensor, the equivalent mass written as$m_{cl,1}$,the second equivalent mass$m_{cl,2}$is some linkage behind of force sensor and joystick. Elastic coefficient of force sensor is k. Mathematical model of the operating mechanism is equation (1).

$$\begin{cases} m_{cl,1}\ddot{x}_1 = -B_{cl,1}\ddot{x}_1 - kx_1 + kx_2 - f_1 + F_c \\ m_{cl,2}\ddot{x}_2 = -B_{cl,2}\ddot{x}_2 + kx_1 - kx_2 + F_{tl} \\ X_{sl} = x_2 \\ F_{se} = k(x_1 - x_2) \end{cases} \tag{1}$$

All the variables in equation (1) are converted to the force sensor variables discard mechanical clearance,$F_{tl}$is the driving force. $F_{se}$is force detected from sensor. $X_{cl}$is operation displacement. $f_i$is the frictional forces acting on the mass i, f_1 plays a dominant role among them. $B_{cl,i}$is damping coefficient of operating mechanism, i=1,2. $F_c$is controllable force of torque motor.

Calculated laplace transform of equation (1) in the initial state when input is zero, we can get the transfer function of the output torque of the motor to the force sensor output, and the format is equation (2) and (3).

$$F_{se} = G_{11}(s)(F_c - f_1) + G_{12}(s)F_{tl} \tag{2}$$

$$G_{1i}(s) = \frac{k_i(\tau_{n,i}S+1)}{\tau_3 s^3 + \tau_2 s^2 + \tau_1 s + 1}, k_i < 1, i = 1,2 \tag{3}$$

discrete the above equation, we can get Z transform(equation (4)) from controlled variable tomeasurementvariable.

$$\frac{F_{se}(z)}{F_c(z)} = z^{-2}\frac{b_0 + b_1 z^{-1}}{1 + a_1 z^{-1} + a_2 z^{-2} + a_3 z^{-3}} \tag{4}$$

In the case of safety, pulse force input in positive and negative direction which generated by 4 grade M sequences was loaded to operating mechanism at a position within stroke, the pulse period is 0.1s, operating mechanism will move back and forth within a certain stroke,collected 0~N the motor command, encoder data and Force feedback signal in movement. According to the encode data and the friction prior information, did friction compensation in the control variables, the motor output torque value after compensation as the input of the system, estimated the unknown parameters in equation (4).

Assume the unknown coefficients$a = [a_1 a_2 a_3 b_0 b_1]^T$, the least square procedure can be used to obtain the unknown parameters.

$$a = (\emptyset^T \emptyset)^{-1} \emptyset^T Y \tag{5}$$

In equation (5), $\emptyset = \left[F_{N-1}{}^T F_{N-2}{}^T \cdots F_3{}^T \right]^T$, $Y = [F_{se}(N-1)]^T [F_{se}(N-1)]^T \cdots [F_{se}(3)]^T$, $F_k = [-F_{se}(k-1) - F_{se}(k-2) - F_{se}(k-3)F_c(k-2)F_c(k-3)]^T$, substituteda into the formula (4) after we get it, and calculated Z inverse transformation, so we can get the frequency domain model of the object that we need[6].

2.3. System Control Strategy

Since the force sensor of the inner loop installed in the connecting rod between the torque motor and steering column, so the force that driver 's hand feeling by manipulating the stick is not exactly the same as the input force on force loop, which is joined by the force on force sensor and the friction of drive mechanism. Because there is a gap in the drive mechanism, the bandwidth of the system is too high to produce limit cycle, embodied a higher frequency oscillation [7-8]. In order to reduce the requirement of the system response bandwidth, the desired load force directly fed to the input of the torque motor.

Steering control system block diagram is shown in Figure 3, $C_p(X)$ is the nonlinear load curve nominal value in Figure 2. Known from (1), $P_i(s) = \dfrac{1}{m_{cl,i}(s + \frac{B_{cl,i}}{m_{cl,i}})}$ in Figure 3.
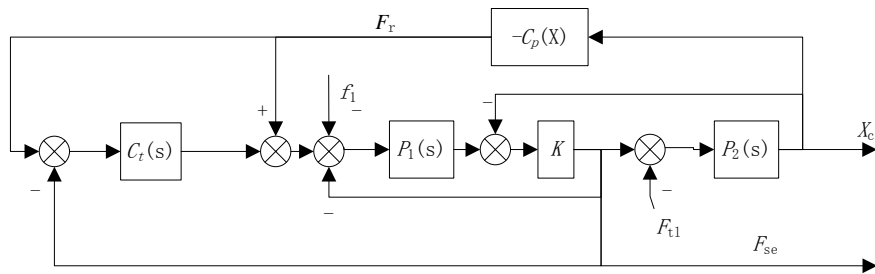

Figure 3. Force Control System Block Diagram

In order to make the hand feeling as far as possible with the expected loading curve, let F_{se} be a feedback and compared with the expected load curve, the error was put into the controller $C_t(S)$ that will be designed, adjust the torque output of the motor, to achieve the purpose of interference suppression [9-11].

By the second formula of equation (1), for a fixed force input, there is equation (6) when the system is stable.

$$-F_{se} = F_{tl} \tag{6}$$

Set the desired output $F_r = -C_p(X_{cl})$, so the control variable $F_e = C_t(S)(F_r - F_{se}) + F_r$, substitution into formula(2), $F_{se} = G_1(s)F_r - G_2(s)f_1 + G_3(s)F_{tl}$, among them $G_1(s) = \dfrac{G_{11}(s)(1+C_t(s))}{1+G_{11}(s)C_t(s)}$, $G_2(s) = \dfrac{G_{11}(s)}{1+G_{11}(s)C_t(s)}$, $G_3(s) = \dfrac{G_{12}(s)}{1+G_{11}(s)C_t(s)}$. The system reaches steady state, from equation (3), there is the integral containing in $C_t(S), G_1(0) = 1, G_2(0) = G_3(0) = 0$, with $F_{se} = F_r = -C_p(X_2)$, note at this point formula (6) is also established which can be balance to satisfy the $F_{tl} = C_p(X_{cl})$ stroke position constrained in graph (2), as long as $C_t(S)$ make the system stability that shown in Figure 3. The system in Figure 3 was transform into the form in Figure 4. In order to make the controller containing integrating element, sensitivity function should append approximate integral weighted $W_v(S) = (s + 1/\tau_s)/(s +$

$\varepsilon)/(1+p)$, $P > 0$, $\varepsilon \to 0 +$. Considering the system has large uncertainty in high frequency, in order to guarantee the system robust stability, the weighted W_e on the output of F_{se}, the weighted W_u on the controlled variable u, these two weight functions are high pass characteristics. The system contains the under damped link, if use multiplicative or additive uncertainty description, conservatism is too high, therefore the uncertainty model is divided into two parts, the unmodeled dynamics is described by W_e, the uncertainties of the under damped link was described by parameter uncertainty.

In general, the dead zone is near the origin point, nonlinear outside of dead zone meet $k_2 x_2 < C_p(x_2) < k_1 x_2$, let $\Delta_k = \frac{k_1 - k_2}{k_1 + k_2}$, $k_n = \frac{k_1 + k_2}{2}$, and $|\Delta_k| < 1$. So $|C_p(x)| < |k_n(1 + \Delta_k)x|$, because $m_{cl,2} \ll m_{cl,1}$, in low frequency $G_{12} \approx G_{11}$, starting from the disturbance on system performance, the weighted f_1 is consistent with F_{tl} for the sake of convenience, do the simplified as Figure 4. Let $z = [z_1 z_2]^T$, $w = [w_1 w_2]^T$, in the case of not cause confusion, simplify transfer function $G(s)$ as G (the same below), the augmented object transfer function matrix as shown in the following equation: $\begin{bmatrix} z \\ y \end{bmatrix} = \begin{bmatrix} G_{zw} G_{zu} \\ G_{yw} G_{yu} \end{bmatrix} \begin{bmatrix} w \\ u \end{bmatrix}$, among them, $G_{zu} = \frac{G_{11}}{1 + G_{11} k_n P_2} \begin{bmatrix} -k_n P_2 \\ W_e \end{bmatrix}$, $G_{zw} = G_{zu}[1 \quad W_d]$, $G_{yu} = -\frac{(1 + k_n P_2) G_{11}}{1 + G_{11} k_n P_2}$, $G_{yw} = [1 \quad 0] + G_{yu}[1 \quad W_d]$, the above equation was rewritten as state equation (7).

$$\begin{cases} x = Ax + B_1 w + B_2 u \\ y = C_1 x + D_{11} w + D_{12} u \\ z = C_2 x + D_{21} w + D_{22} u \end{cases} \tag{7}$$
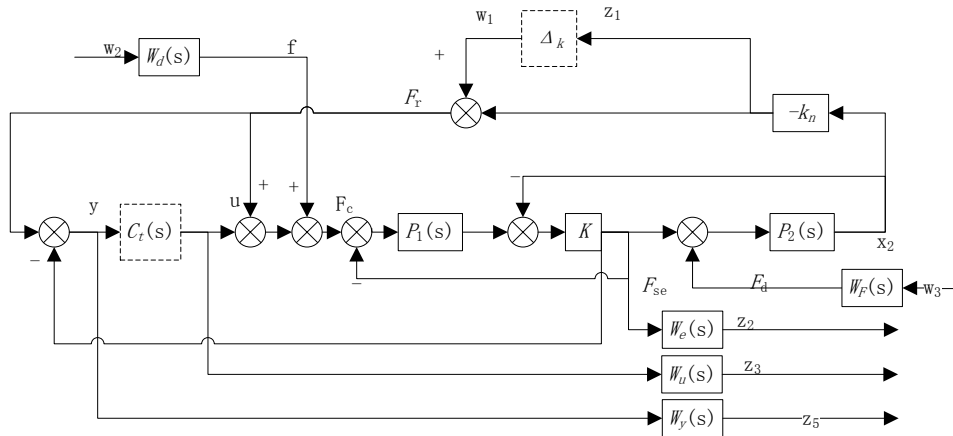

Figure 4. Augmentation Object Model

According to the bounded real lemma, about linear constant system as above formula, for any $\|\Delta\|_\infty \leq 1$ has an H$_\infty$ output feedback controller such that the necessary and sufficient conditions for $\|T_{zw}\|_\infty < 1$ is that: if and only if there exists symmetric positive definite matrix X and Y, and make equation (8),(9) and (10) established.

$$\begin{bmatrix} N_0 \\ I \end{bmatrix}^T \begin{bmatrix} A^T X + XAXB_1 C_1^T \\ B_1^T X - ID_{11}^T \\ C_1 D_{11} - I \end{bmatrix} \begin{bmatrix} N_0 \\ I \end{bmatrix} < 0 \tag{8}$$

$$\begin{bmatrix} N_c \\ I \end{bmatrix}^T \begin{bmatrix} AY + YA^T Y C_1^T C_1^T B_1 \\ C_1 Y - ID_{11} \\ B_1^T C_1 D_{11}^T - I \end{bmatrix} \begin{bmatrix} N_0 \\ I \end{bmatrix} < 0 \tag{9}$$

$$\begin{bmatrix} X & I \\ IY & \end{bmatrix} \leq 0 \tag{10}$$

In equation (8), (9) and (10), N_0 and N_c are matrix formed by any of a group of base vector as a column vector of subspace $ker([C_2 D_{21}])$ and $ker([B_2^T D_{12}^T])$. (A, B_2, C_2) is stable and can be detected, $D_{22} = 0$, there is a output feedback controller, the state space expression is equation (11).

$$\begin{cases} \dot{\hat{x}} = A_K \hat{x} + B_K y \\ u = C_k \hat{x} + D_K y \end{cases} \tag{11}$$

The output feedback controller make the closed-loop system asymptotically stable, and $\|T_{zw}(s)\|_\infty < 1$, the controller parameter matrix is equation (12).

$$K = \begin{bmatrix} A_K B_K \\ C_K D_K \end{bmatrix} \tag{12}$$

Calculated as follows:

(1) to compute matrix X_2 for meet $X - Y^{-1} = X_2 X_2^T$.

(2) make: $A_0 = \begin{bmatrix} A & 0 \\ 0 & 0 \end{bmatrix}, B_0 = \begin{bmatrix} B_1 \\ 0 \end{bmatrix}, C_0 = [C_1 \quad 0], \bar{B} = \begin{bmatrix} 0 & B_2 \\ I & 0 \end{bmatrix}, \bar{C} = \begin{bmatrix} 0 & I \\ C_2 & 0 \end{bmatrix}, \bar{D}_{12} = [0 \quad D_{12}],$

$\bar{D}_{21} = \begin{bmatrix} 0 \\ D_{21} \end{bmatrix}, X_{cl} = \begin{bmatrix} X & X_2^T \\ X_2 & I \end{bmatrix}$, the coefficient matrix of the closed loop transfer function matrix respectively is: $A_{cl} = A_0 + \bar{B}K\bar{C}, B_{cl} = B_0 + \bar{B}K\bar{D}_{21}, = C_0 + \bar{D}_{12}K\bar{C}, D_{cl} = D_{11} + \bar{D}_{12}K\bar{D}_{21}$.

(3) make: $H_{cl} = \begin{bmatrix} A_0^T X_{cl} + X_{cl} A_0 X_{cl} B_0 C_0^T \\ B_0^T X_{cl} & - I D_{11}^T \\ C_0 D_{11} - I \end{bmatrix}, P_{Xcl} = [\bar{B}^T X_{cl} \quad 0 \quad \bar{D}_{12}^T], Q = [\bar{C}\bar{D}_{21} \quad 0],$

according to the bounded real lemma, the necessary and sufficient conditions for the closed-loop system asymptotically stable and $\|T_{zw}(s)\|_\infty < 1$ is: existing matrix K such that equation (13) was established.

$$H_{cl} + P_{Xcl}^T KQ + Q^T K^T P_{Xcl} < 0 \tag{13}$$

Equation (13) is the linear matrix inequalities of matrix K, solution of K, from equation (12), K is the H_∞ output feedback controller [12, 13]. After balanced reduction, we can obtain the feasible controller order lower.

3. Simulation Analysis

The simulation parameters are selected as shown in the following table.

Table 1. Simulation Parameters

$m_{cl,1}$/kg	$m_{cl,2}$/kg	$B_{cl,1}$/Ns/m	$B_{cl,2}$/Ns/m	K/N/m	ε
35	8	80	8	$(1 \pm 10\%) \times 8 \times 10^{-4}$	1×10^{-4}

The weighting function is selected as the following: $W_d = \frac{1}{20}, W_F = \frac{1}{0.083s+1}$, $W_e = \frac{0.05(0.0083s+1)}{0.0005s+1}$, taking into account the uncertainty of the resonant frequency of the system, it's too conservative if use the multiplicative or additive modeling features to express, described by parameter uncertainty, the changes of object bode caused by 10% of the elastic parameters perturbation are shown in the following Figure 5.
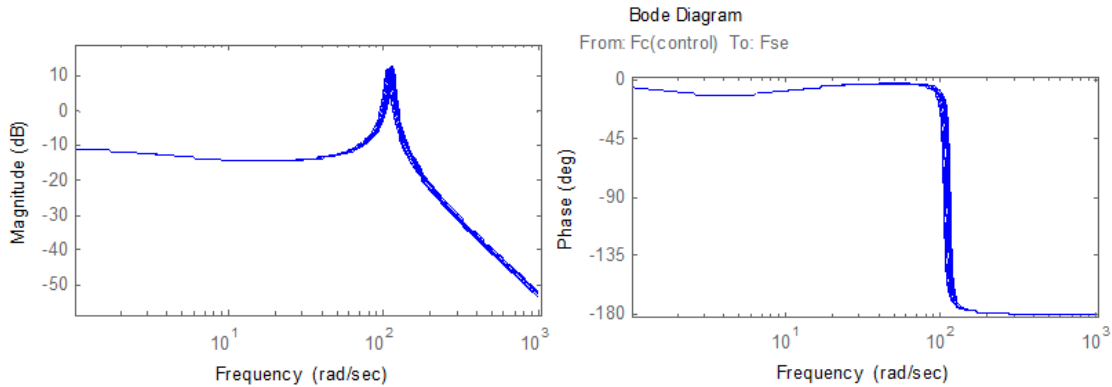
Figure 5. Control Object Bode Diagram with Parameter Uncertainty

Comprehensive result of controller is equation (14).

$$C(t) = \frac{41864(s+3.614)(s+0.2361)(s^2+33s+347.4)(s^2+23.46s+9764)}{s(s+600)(s^2+6.713s+62.17)(s^2+4.085s+187.4)(s+1043)} \tag{14}$$

After the controller is added to the system, the nominal open-loop cutting frequency is 170 rad/s, phase margin is 49.5°. Since the object resonance point is uncertain, therefore the comprehensive results of the controller did not produce a fully cancellation case of the pole-zero, but bring about the two pairs of poles to suppress the effects of vibration modes. After adding the controller, open loop bode diagram and nyquist curve with the object parameter uncertainty is shown in Figure 6, it can be seen from the nyquist plot, the system frequency characteristic curve does not encircle -1 point, and from that point there is enough distance.


a) Bode Diagram   b)Nyquist Curve
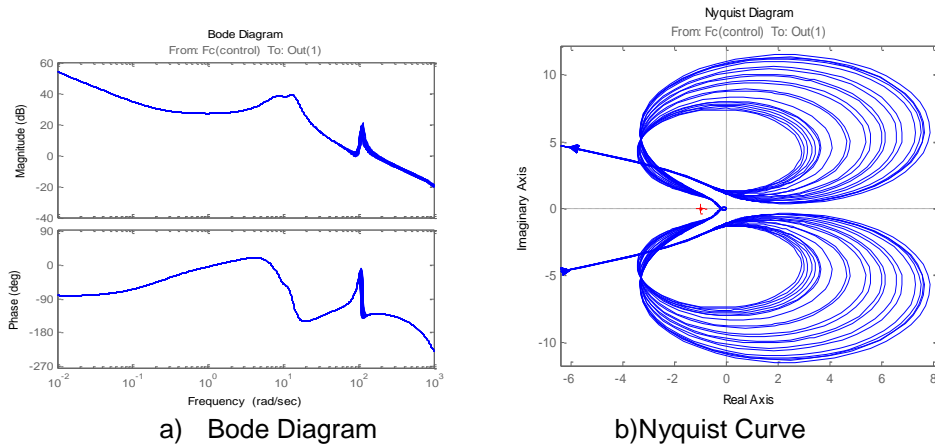
Figure 6. Character of Open-loop Control System

After the system is closed-loop ,the bode that response to the thrust command is shown in Figure 7, where the solid line is the tracking characteristics of the inputting thrust, the broken line is the tracking error characteristic. As seen from the figure, in the required bandwidth the tracking error to pressure command is small, and when the frequency is too high track will not be completely keep up. The closed loop bode of the suppression to friction interference is shown in Figure 8. Further analysis about the worst case shows that system occurs at the worst case in 14.4rad/s, where reachedH_∞norm bounded 1.09.
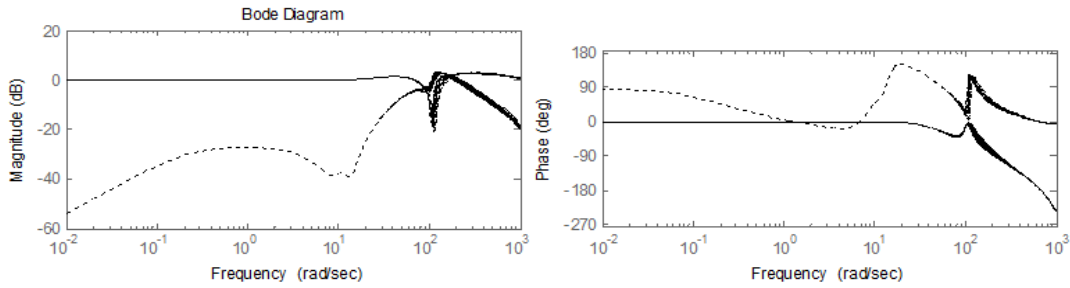
a. Given Force Follow Actual Force   b. Force Err

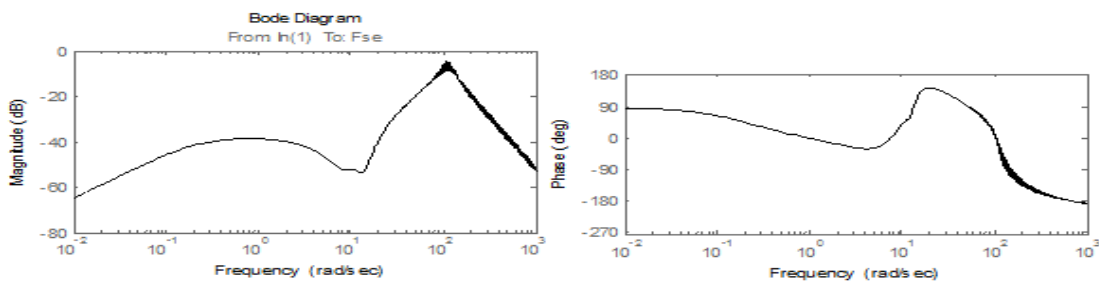**Figure 7. Frequency Characteristics of Given Force Following the Actual Forcer**

Figure 8. Closed-loop Bode Diagram of Friction Interference Suppression

In order to verify the controlling performance, system simulation diagram was build using simulink software and shown in Figure 9. The friction is coulomb friction, the size is 10N, the input force of joystick is sinusoidal signal that shown in Figure 10, and the amplitude is 200N. The given force is divided into three sections, the gain of first section is 800N/m, and the second section gain is 500N/m, the gain of third section that closed to stroke boundary is 1500N/m. The simulation result shown in Figure 11. Where the center of the red line is the desired reaction force, the blue line is the actual reaction force, the difference between the two shown in Figure 12. So the control system can be stabilized, and the actual thrust-displacement curve and the desired curve within an allowable error range.
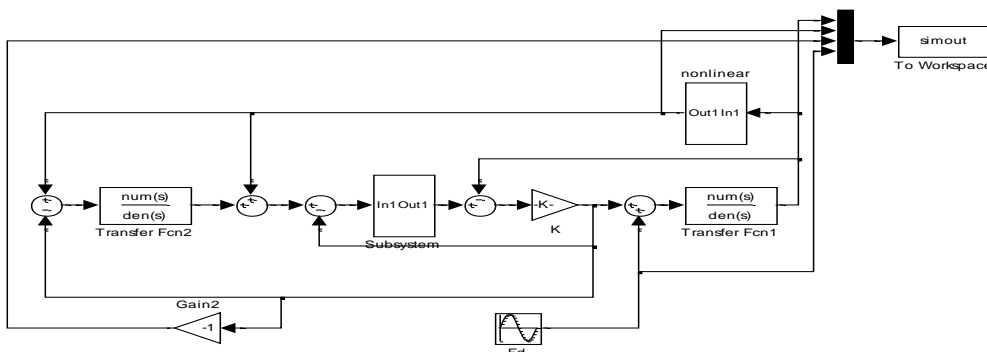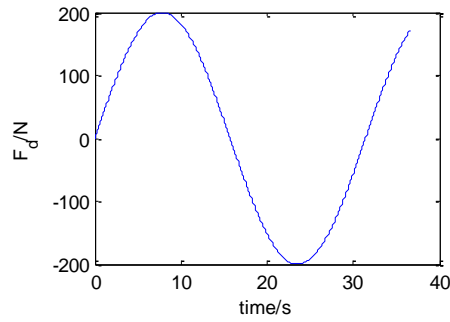

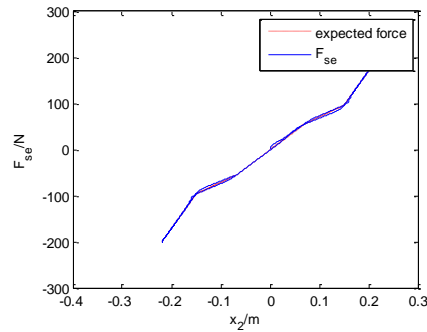**Figure 9. Simulink Simulation Block Diagram**

Figure 10. Operating Mechanism Force
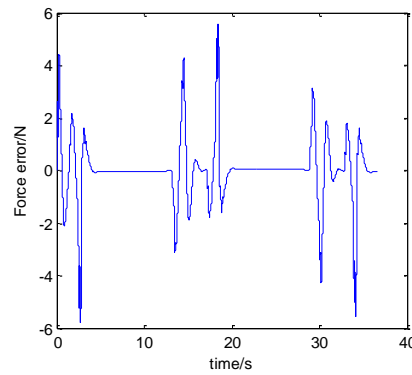

Figure 11. Force Displacement Curve

Figure 12. Force Difference of Expectation and Feedback

4. Experimental Verification

Figure 13 is a control loading system test bench of a fighter stick (dual channel), the structure of the two channels are shown in Figure 1-a, the position feedback used the encoder which belong to the servo motor. After repeatedly adjust the controller parameters, we tested the static and the dynamic force characteristics of a channels.
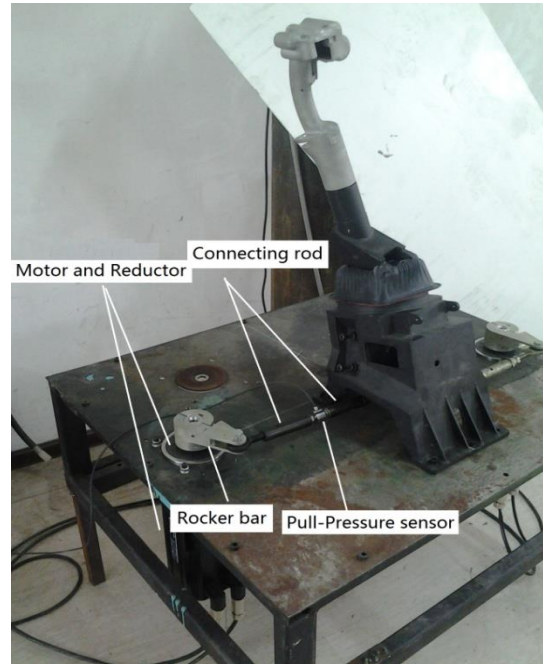
Figure 13. Control Loading System Experimental Bench

Static force test: the aircraft was placed in the ground status in the position loop (outer loop), the force - displacements curve was shown in Figure 14, the actual force and the given force was consistent. The difference force between the forward stroke and reverse stroke is approximately equal to twice of the friction.
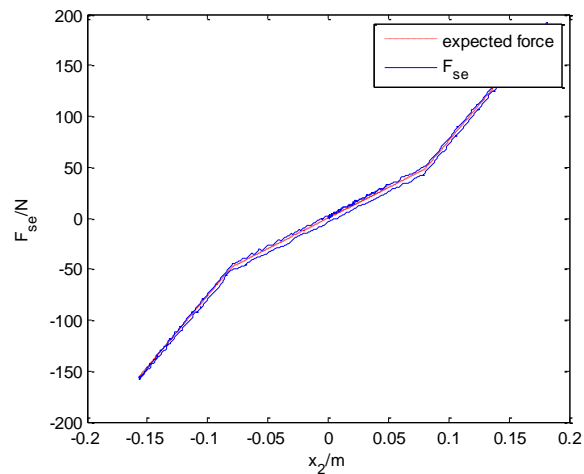

Figure 14. Static Stroke Force Curve

Dynamic force test: the aircraft was placed in a certain height and speed status in the position loop, manipulated the stick in full stroke and made aircraft closed to maximum pitch, the time-force curve was shown in Figure 15, Figure 16 isforce error curve, the maximum error of force was about 5N, the actual force followed preciselythe given force.
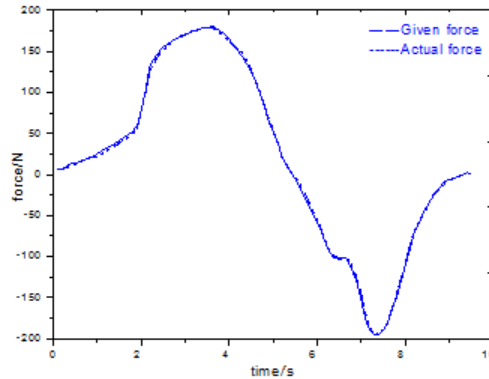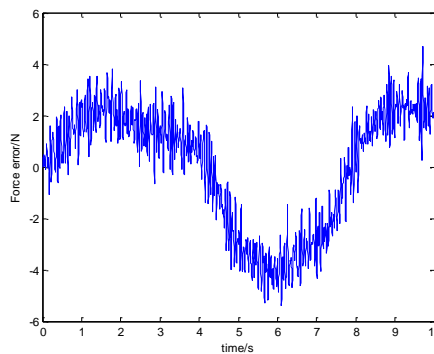
Figure 15. Given Force and Actual Force Curve

Figure 16. Force Error Curve

5. Conclusion

Flight simulator adopts motor type electric control loading system is the development direction of the future. For single input single output electric control loading system, using the classical control theory can obtain a good control performance, the controller based on the LMI (linear matrix inequality) was applied to a control loading system of a flight simulator, the simulator operating system reproduce realistic the real driving force sensing characteristics of real plane. The electric control loading system has been equipped in a plurality of flight simulator, the system has high performance price ratio.

References

[1] X. Wang, "Real-time Flight Simulation System and Technology", Beihang University Press, **(1998)**.
[2] A. Gerretsen, M. Mulder and M. M. van Paassen, "Comparison of position-loop,velocity-loop and force-loop based control loading architectures", AIAA Modeling and Simulation Technologies Conference and Exhibit.Reston,VA,USA:AIAA, **(2005)**, pp. 50-59.
[3] H. Wang, X. Yan, L. Wang and J. Guo, "Comparison Research on Control Methods of Electro- hydraulic Servo Loading of Control Loading System", China Mechanical Engineering, vol. 18, **(2007)**, pp. 142-145.
[4] J. Zhao, Z. Ye, G. Shen and J. Han, "Inverse Model Control for Inner Loop of Control Loading System on Flight Simulator", Academic Journal of Xi'an Jiaotong University, vol. 46, **(2012)**, pp. 3 8-44.
[5] P. Qi, "Force-feel cueing study of hydraulic control loading system of flight simulator", Harbin Institute of Technology, **(2009)**.
[6] P. Zhonghua and C. Hong, "System identification and adaptive control MATLAB simulation", Beihang University Press, Beijing, China, Harbin, China, **(2009)**.

[7]   S. Sakaino, T. Sato and O. Kouhei, "Force-based disturbance observer for dynamic force control and a position/force hybrid controller", IEEJ Transactions on Electrical and Electronic Engineering, vol. 8, **(2013)**, pp. 505-514.

[8]   N. Yoonsu, "Dynamic characteristic analysis and force loop design for the aerodynamic load simulator", Journal of Mechanical Science and Technology, vol. 14, **(2012)**, pp. 1358-1364.

[9]   X. D. Shi, F. Zhang, T. Jing and D. Y. Li, "Control and simulation of electric control loading system of flight simulator", Electric Machines and Control, vol. 14, **(2010)**, pp. 73-78.

[10]   N. Yoonsu , J. Lee and S. K. Hong, "Force control system design for aerodynamic load simulator", Control Engineering Practice, vol. 10, **(2002)**, pp. 549-558.

[11]   M. Karpenko and N. Sepehri, "Electrohydraulic force control design of a hardware-in-the-loop load emulator using a nonlinear QFT technique", Control Engineering Practice, vol. 20, **(2012)**, pp. 598-609.

[12]   G. Jinfeng, Y. Li and C. Wang, "LMI and Applications in Control Engineering", control engineering, vol. 10, **(2003)**, pp. 145-148.

[13]   Z. Hu, S. Shi and Z. Weng, "Application and Development of Linear Matrix Inequality in Control Theory", Journal of ShangHai JiaoTong University, vol. 33, **(1999)**, pp. 1458-1461.

Author

Yuping Wang, she was born in Heilongjiang province, China on November 1979. She received her bachelor degree in Electrical engineering received her master degree in Control theory and control engineering, Heilongjiang University of Science and Technology, Harbin. Her research is mainly in power electronics and power transmission.